Feature Extraction and Selection for EEG and Motion Data in Tasks of the Mental Status Assessing
Pilot Study using Emotiv EPOC+ Headset Signals

Alexey Syskov, Vasilii Borisov, Vsevolod Tetervak and Vladimir Kublanov

Ural Federal University named after the first President of Russia B.N. Yeltsin, 19 Mira str., 620002, Yekaterinburg, Russia

Keywords: Accelerometer, Brain-Computer Interface, Electroencephalography, Machine Learning, Mental Evaluation, Test of Variables of Attention, Principal Component Analysis.

Abstract: In the paper the results of extracting and selection the features of EEG data and accelerometer for mental status evaluation are shown. We have used 14 channel wireless EEG-system Emotiv EPOC+ with accelerometer (motional data - MD) for short-term recording under several functional states for 10 healthy subjects: Functional rest (rest state), TOVA-test (mental load), Hyperventilation (physical load) and Aftereffect (after test state). We then extracted core features from EEG-only and MD-only data using principal component analysis. After that, supervised learning methods were used for mental state classification: EEG-only core features for AF3, T7, O1, T8, AF4 channels, MD-only core features and EEG- MD integrated core features. Experimental results showed that integrated core features for mental status evaluation have higher prediction accuracy 92,0% for decision tree method.

1 INTRODUCTION

Evaluation of human mental status is a complex and complicated task. Electroencephalography (EEG) is well known method for assessing mental state and optimizing conventional performance: attention; workload; emotion (Wolpaw and Wolpaw, 2012).

Acquisition of EEG signal in real-world conditions is characterized by the usage of mobile and wearables devices (Lin and Jung, 2017; So et al., 2017; Sun et al., 2012). Combinations of different modalities sensors are used for assessing and controlling the subject's function state (Silva et al., 2014).

Accelerometer is one of widely used sensors for assessing body movement artefact during ECG, EEG recording. An accelerometer signal is acquired in order to identify areas of the signal with motion artifacts (Y. Kishimoto et al., 2007). In (Wu et al., 2017) operator's mental workload is measured with EEG headset. EEG headset was composed of two electrodes and an accelerometer attached to the electrodes. When in some epoch the acceleration of the electrodes exceeds a certain value, EEG data corresponding to that epoch were removed from further analysis.

Moreover, there are few works where accelerometer-only data were used to study neurological diseases (Kutilek et al., 2010). In (Danilov et al., 2008) the vestibular system is considered as important in virtually every aspect of our daily life. Head acceleration information is essential for our adequate behavior in three-dimensional space not only through vestibular reflexes that act constantly on somatic muscles and autonomic organs, but also through various cognitive functions such as perception of self-movement, spatial perception and memory, visual spatial constancy, visual object motion perception. Thus, accelerometer data can be used for subject's functional state classification in combination with other sensors.

A small and light-weight wearable electrocardiograph (ECG) equipment with a three-axis accelerometer (x, y and z-axis) was developed for prolonged monitoring of everyday stress (Okada et al., 2013). In that study, the waveform of acceleration data were used as the pattern for a subject's movement or posture in long-term monitoring. In (Wu et al., 2015) two modalities of sensors: HRV recorders and accelerometers were integrated to monitor the stress levels in daily life. The accuracy of stress level classification was

improved by 4.9% on average in comparison with HRV-only feature set. Therefore, accelerometer data can be used in long-term monitoring as tool to identify areas of the signal with motion artifacts and subject's activity classify.

In our paper, we have used the Emotiv EPOC+ head set for gathering both motion and EEG data in short-term experiments under several functional states. The aim of the study is evaluation of feature in EEG-only, accelerometer-only and integrated feature spaces in series of short-term experiments.

2 MATERIALS AND METHODS

A series of experiments with headset Emotiv EPOC+ was carried out to study parameters which would describe different subject mental status. The Emotiv EPOC + headset provides information about the induced electrical activity of the brain from 14 channels (David et al., 2014). This information contains the voltage value for each electrode with a sampling frequency of 128 Hz. Figure 1 depicted the layout of the electrodes is AF3, F7, F3, FC5, T7, P7, O1, O2, P8, T8, FC6, F4, F8, AF4 in standard 10-20 scheme. In addition, the motion data from three-axis accelerometer integrated into the headset were collected.

Each experiment contained five stages as presented in Table 1. During each of the stages the subject sits opposite the PC monitor and looks at the screen with instruction and tasks.

Table 1: The cyclorama of the experiment.

Stage	Duration, sec
1. Rest state (RS)	300
2. TOVA test (T1)	180
3. Hyperventilation load (HL)	180
4. TOVA test (T2)	180
5. Aftereffect (AE)	300

Recording the stage of rest state involves biomedical signals data from the subject, who looks at the black screen and does nothing.

The next stage is carried out with the TOVA test, which is the test of attention of variability - a psycho-physiological test to evaluate conventional performance related to attention and control of the reaction. The Pebl software was used for the test procedure. During the test squares and circles appears alternately at the top and bottom of the computer screen. The task of the subject is to press a space on the keyboard when a square appears at the top of the

screen (Mueller and Piper, 2014).

The stage of hyperventilation is standard functional load, when the subject often breathes throughout the entire length of time, simulating breathing during heavy sport loads.

Collected in each experiment raw EEG and accelerometer data were saved into storage with additional information about the subjects and events marks (Borisov et al., 2017).

2.1 EEG Feature Engineering

Collected during the experiments raw EEG data were processed in several steps of feature extraction and selection. The process of feature engineering is presented in Figure 1.
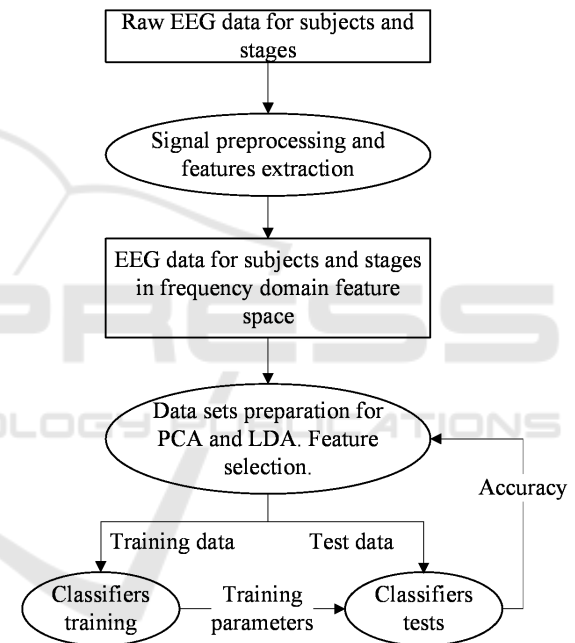

Figure 1: EEG feature engineering.

In the first step, all EEG data were transformed to the frequency domain. To separate EEG – rhythms from the signal, a second-order Butterworth bandpass filter were applied. Rhythms borders were: Theta (4-7) Hz, Alpha (7-15) Hz, Beta-Low (15-25) Hz, Beta-High (25-31) Hz. Discrete Fourier transform method was used for frequencies' magnitudes extraction. As result, four coefficients are calculated for each of 14-th channel. Each coefficient is sum of magnitudes for one of the rhythms. Thus, EEG data in frequency domain are described as 56-dimension feature space.

After that, on the feature selection step (Egorova et al., 2014), principal component analysis method (PCA) (Jolliffe, 2014) in combination with linear

discriminant analysis (LDA) (McLachlan, 1992), are used for reducing 56-dimension feature space. Data sets for analysis contained EEG recordings for all subjects and the following pairs of stages: RS and HL; RS and T1; T1 and HL.

LDA was used for evaluation of the principal components pairs (Kublanov et al., 2016). The pair of components with best accuracy and maximum described variance were selected as base for new feature space.

Finally, information about PCA loadings were used for selecting EEG channels and frequency bands as EEG new feature space. After that, supervised learning methods were used for mental state classification.

2.2 Accelerometer's Feature Space

The Emotiv EPOC + headset, in addition to information about the induced electrical activity of the brain, provide data from a three-axis accelerometer, which allows assessing the movement of the headset in space during the experiment. Accelerometer data is recorded to a separate file, each record contains the values of the acceleration for each axis and the data recording time. The scheme of the accelerometer axis is shown in Figure 2.
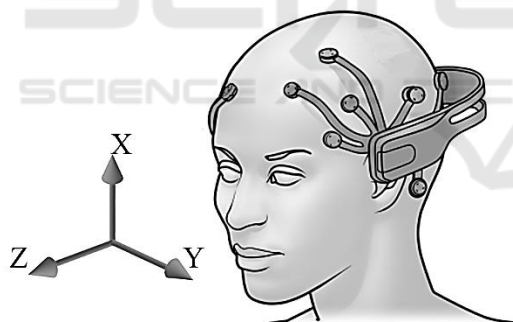

Figure 2: Accelerometer axis orientation ("EMOTIV Epoc - 14 Channel Wireless EEG Headset," n.d.).

The three-axis accelerometer provides information on the magnitude of the acting accelerations along the three axes, respectively. The acceleration value for each axis is registered through equal time intervals. The signal measured by the accelerometer is a linear sum of three components (Machado et al., 2015):

- Body Acceleration Component (BA) is acceleration resulting from body movement;
- Gravitation Acceleration Component (GA) is acceleration resulting from gravity;
- Noise inherent to the measuring system.

GA provides information about the spatial orientation of the device, and the BA provides information about the movement of the device and subject's head movement. The frequency spectrum of accelerations caused by human motion is located in the range from 0 to 20 Hz. The gravitational component is located in the range from 0 to 0.3 Hz.

The component containing instrumental noise is located generally in the range above 20 Hz. To isolate the motion component from the signal, a second-order Butterworth window filter with frequencies from 0.3 to 20 Hz was applied (Mathie, 2003). In Figure 3 the accelerometer signals before and after filtering are represented. According to the article (Wu et al., 2015), the most revealing motion data (MD) features of the accelerometer signal are present in Table 2.

Because of the discrete nature of the accelerometer signal, ZCR was calculated as the number of sections where the previous sign differs from the current sign.

Activity - the value characterizing the change in the signal over time was calculated by the following formula (2):

$$Activity = \sum_{i=1}^{n} \sqrt{\Delta_x{}^2 + \Delta_y{}^2 + \Delta_z{}^2}, \qquad (1)$$

where $\Delta_x = (x_i - x_{i-1})$;
x_{i-1}, x_i are consecutive counts for x axis;
Δy, Δz are calculated in same way for y and z axles

The average activity time is the ratio of the total activity time, which exceeds the average level by 10%, to the number of stages exceeding this level. The level of 10% was chosen as the most informative.

After calculating all features for each subject, the data was written into the matrix F by N, where F is the number of features, and N is the result of multiplication the number of stages by the number of subjects.

3 RESULTS

The results of feature selection for EEG in different data sets are shown in section 3.1.

In section 3.2 results of classification for EEG-only feature, accelerometer-only feature and integrated feature space are shown.
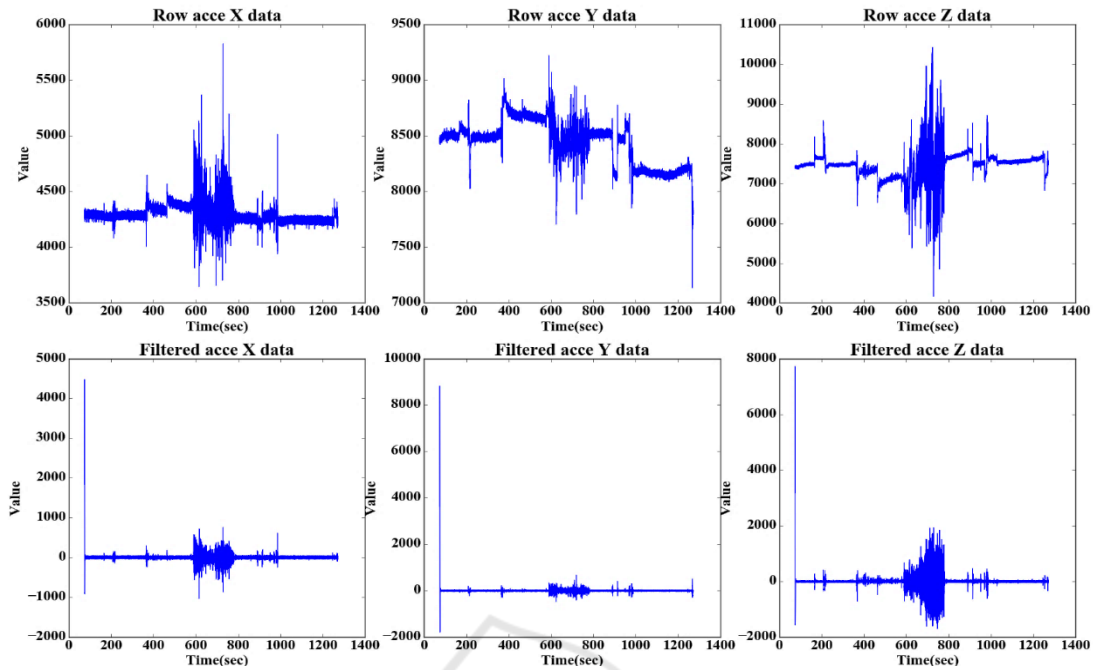
Figure 3: Accelerometer axes signal before and after filtering.

Table 2: MD features of the accelerometer signal.

MD feature	Description
	Axis features
Max	Maximum value is the maximum acceleration value at a given time interval
Min	Minimum value is the minimum value of acceleration at a given time interval
Average value	The average value of acceleration at a given time interval
STD	Indicates the dispersion to the mean of the signal over time a given time interval
ZCR	Zero cross rate is the number of intersections by the zero signal.
Energy	Signal energy at a given time interval
	Non axis features
Mean ZCR	Mean zero cross rate for three axes for current stage
Mean Energy	Mean energy for three axes for current stage
Activity	Characteristic of signal change
Average activity time	Mean time of high-level activity

3.1 EEG Feature Selection

Here we show the results for all subjects and combination of stages in the following pair of data sets:

1. HL and RS;
2. T1 and RS;
3. T1 and HL.

3.1.1 Hyperventilation Load and Rest Data Set

Figure 4 depicted cumulative sum of variance for principal components. The first two components explained 82% of total variance.
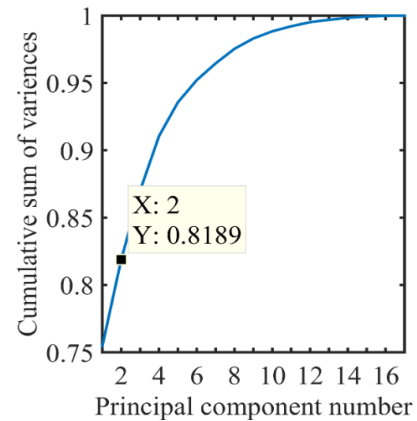

Figure 4: Cumulative sum of variance for HL and RS.

After that, a classification was performed using LDA for component 1 and 2. Training data contains 9 subjects for two classes RS and HL (functional rest and hyper ventilation load).

Next step we calculate the prediction accuracy estimation on an independent data sets by doing cross-validation. During iterative procedure, we remove one of the subject in training set. Figure 5 shows the result of classification. The average accuracy of classification 94%.
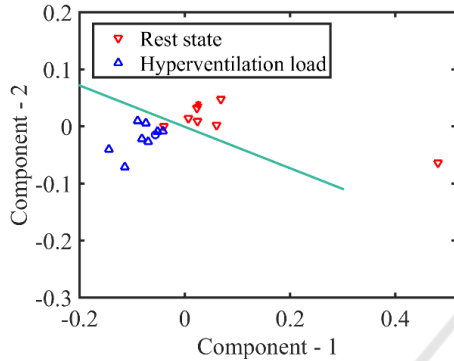

Figure 5: Classification of subjects for HL and RS.

We used the equation (2) for interpretation of LDA linear coefficients, where K – vector of constant, L – vector of linear coefficients, v – data vector.

$$K + L*v = 0 \qquad (2)$$

Figure 6 presents stats boxes for normalized linear coefficients L from (2) for independent sets for PCA scores 1 and 2. Component N-2 more significant for discrimination on data set with two classes of RS and HL.
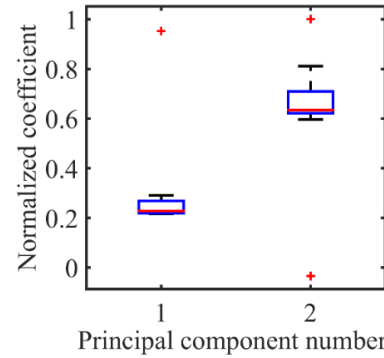

Figure 6: LDA's linear coefficients boxes for HL-RS.

Figure 7 (a) represents image plot of PCA-loadings. Loadings are structured along the channels and rhythms of the EEG. For each channel, the values for Theta, Alpha, Beta-low and Beta-High EEG-rhythms are presented. The EEG-rhythms order is shown in the figure. The values of the loading are normalized and a color scale is introduced.
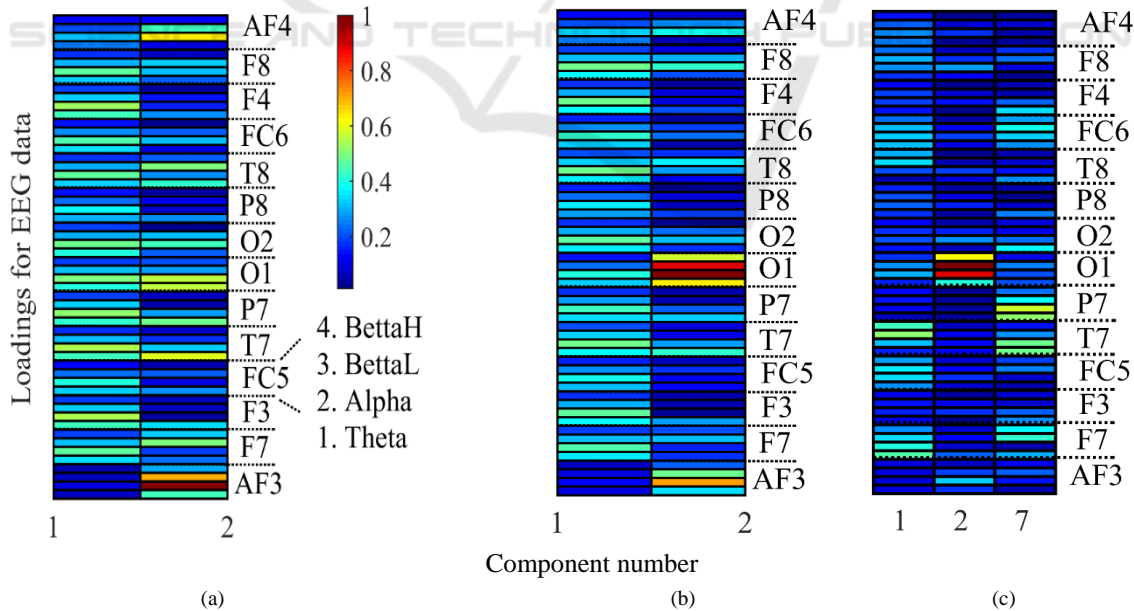

Figure 7: Normalized PCA-loadings image plots.

a) – image plot of PCA-loadings for HL and RS data set;
b) – image plot of PCA-loadings for T1 and RS data set;
c) – image plot of PCA-loadings for T1 and HL data set.

First component reflects variance caused by Theta and Alpha frequency band activity. Its concerns all EEG channel. Second component reflects variance caused by changing loadings for AF3, P7, T7, O1, T8, AF4 channels.

3.1.2 TOVA and Hyper Ventilation Data Set

Figure 8 depicted cumulative sum of variance for principal components. The first two components explained 86% of total variance.
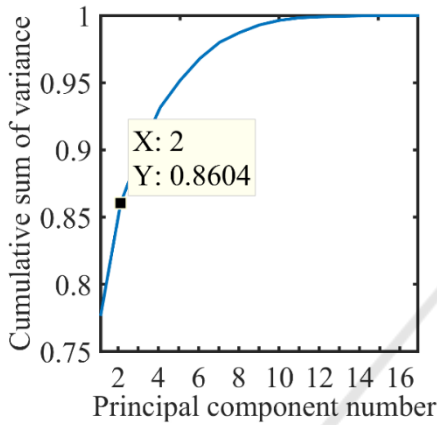

Figure 8: Cumulative sum of variance for HL and T1.

In Figure 9 presented result of linear discriminant analysis on training set for TOVA and rest data set. The average accuracy of classification is 100%.
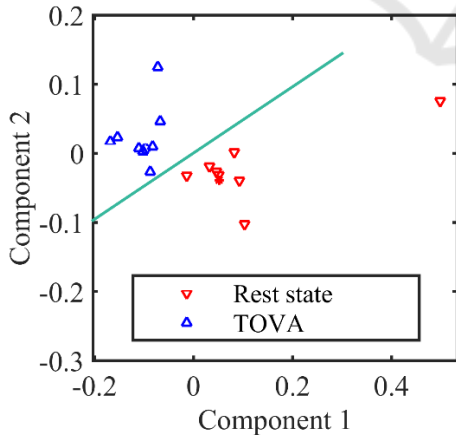

Figure 9: Classification of subjects for RS and T1.

Figure 10 depicts stats boxes for normalized linear coefficients L form (2) for independent sets for components 1 and 2.

As we can see, the both components are equally significant for discrimination on data set with two classes of RS and T1 load.
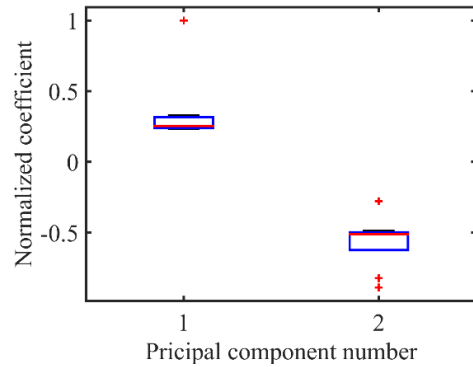

Figure 10: LDA's linear coefficients boxes for T1-RS.

In Figure 7 (b) showed image plot of loadings. First component reflects variance caused by Theta and Alpha frequency band activity. Its concerns all EEG channel. Second component reflects variance caused by changing loadings for AF3 and O1 channels.

3.1.3 TOVA and Hyper Ventilation Data Set

Figure 11 presents cumulative sum of variance for principal components. The first two components explained 61 % of total variance. Sum of variances for 1 and 2 components a sufficient less in comparison with previous cases.
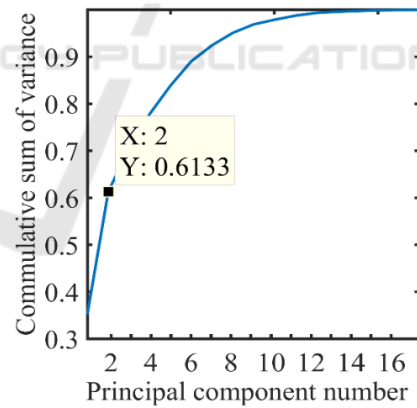

Figure 11: Cumulative sum of variance for HL and T1.

In this case, we try to classify subjects in spaces for all pair combination of components with LDA. The results with accuracy more than 70% depicted in Table 3, where sum of variance for pair based on Figure 12 data, weighted index is multiplication accuracy and sum of variance for pair.

Table 3: Pairs of components, accuracy and sum of variance.

Component pair	Accuracy	Sum of variance for pair	Weighted index
1-7	0.83	0.39	0.32
2-7	0.78	0.29	0.23
1-2	0.72	0.61	0.44

Perform classification using discriminant analysis for 1, 2 components with maximum of weighted index. Figure 13 depicted result of linear discriminant analysis on training set for TOVA and hyperventilation data set.
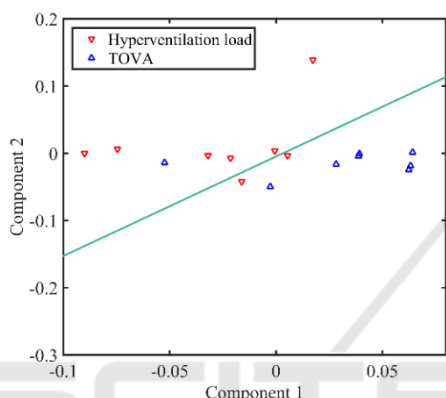

Figure 12: Classification of subjects for HL and T1.

Figure 13 shows stats boxes for normalized linear coefficients L form (1) for independent sets for components 1 and 2. As we can see, the both components are equally significant for discrimination on data set with two classes of RS and T1 load.
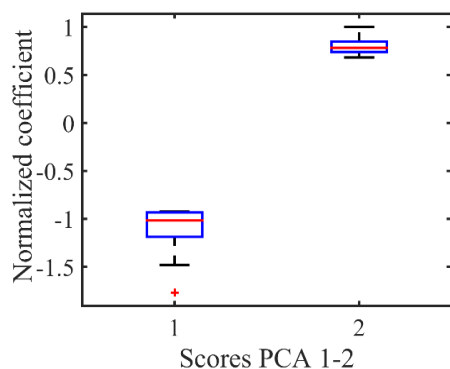

Figure 13: LDA's linear coefficients boxes HL-T1.

Figure 7 (c) presented image plot of loadings. Second component reflects variance caused primary by Alpha and Betta frequency band activity for O1 channel. Channels P7, F7 appears with significant less loadings weights.

3.2 Classification in Integrated Feature Space

Initially EEG feature vector contained 54 components for 14 channels their rhythms borders were: Theta (4-7) Hz, Alpha (7-15) Hz, Beta-Low (15-25) Hz, Beta-High (25-31) Hz. Based on results in section 3.1 AF3, T7, O1, T8, AF4 channels with Theta and Alpha frequency bound are selected for EEG feature space. Integrated features space was created from EEG selected features and accelerometer MD features as showed on Figure 15.
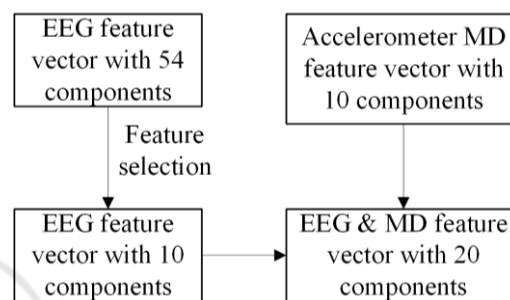

Figure 14: Integrated feature vector.

Full feature space for accelerometer as described in section 2 are used. It need to be mentioned we don't use any weighted coefficients for selected EEG features in model generalization purpose (Wolpaw and Wolpaw, 2012).

LDA, Naïve Bayes (NB) and Decision Trees (DT) classification methods are used for EEG feature space. LDA method applied to finding linear combinations of features that best distinguish object classes. NB method - special case of the Bayesian classifier. The method based on the assumption that the objects are described by the statistically independent variables. DT are nonparametric method. This method does not require any assumptions about the distribution of the variables in each class (Kublanov et al., 2017).

The prediction accuracy evaluated on an independent sets by doing "leave one out" cross-validation (Refaeilzadeh et al., 2009). Table 4 contains the mean accuracy for 10 test data sets for all five stages.

Table 4: Accuracy for EEG and MD feature space.

Method	Accuracy, %		
	EEG-only	MD-only	Integrated
LDA	72.4	89.3	86.7
NB	68.9	89.3	86.7
DT	71.6	84.0	92.0

The best result for integrated feature space have higher prediction accuracy 92.0%, in comparison with EEG-only (72.4 %) mental status evaluation for AF3, T7, O1, T8, AF4 channels. The best results for MD-only data are 89.3% for LDA and NB methods.

4 DISCUSSION AND CONCLUSION

According to the results of the of EEG data analysis for various combinations of functional loads, the most informative channels for Theta and Alpha rhythms in the frontal, hip and occipital areas were identified. For three different classifiers, the best accuracy of classification of the five functional states in the EEG generated characteristic space is at the level of 72.4% for LDA method.

In turn, the classification in the attribute space of the accelerometer, for the LDA and NB classifiers, allows to reach 89.3% accuracy of identification of five functional states. The processing of the joint indicative space of the EEG –MD integrated core features allowed to increase the classification accuracy to 92.0% for DT method.

The results obtained in this paper reflect changes in the power levels of the EEG indices in various functional states, which makes it possible to characterize the functional state of a person. The decrease in the control effect of the cerebral cortex (alpha-rhythm activity) increases the amplitude of the average acceleration of the head movement. The rather high classification accuracy obtained for the signs of EEG signals isolated using the PCA method suggests that changes in physiological processes underlie these changes.

An increase in the accuracy of classification (on 19.6% in comparison with EEG-only feature), when using the characteristics of both feature spaces can mean that each of the signals carries information only about a part of the changes in functional processes.

Thus, the task of determining the relationship between EEG signals and the accelerometer on a wider set of functional samples, when classifying different mental states of a person at short time intervals, is promising.

ACKNOWLEDGEMENTS

REFERENCES

Borisov, V., Syskov, A., Tetervak, V., Kublanov, V., 2017. Mobile Brain - Computer Interface Application for Mental Status Evaluation., in: Proceedings - 2017 *International Multi-Conference on Engineering, Computer and Information Sciences SIBIRCON. Presented at the 2017 International Multi-Conference on Engineering, Computer and Information Sciences SIBIRCON, IEEE*, Novosibirsk, Russia.

Danilov, Y.P., Tyler, M.E., Kaczmarek, K.A., 2008. Vestibular sensory substitution using tongue electrotactile display, in: *Human Haptic Perception: Basics and Applications. Birkhäuser Basel, pp. 467–480.* doi:10.1007/978-3-7643-7612-3_39.

David, H., Whitaker, K.W., Ries, A.J., Vettel, J.M., Cortney, B., Kerick, S.E., McDowell, K., 2014. Usability of four commercially-oriented EEG systems. *J. Neural Eng. 11*, 046018. doi:10.1088/1741-2560/11/4/046018.

Egorova, D.D., Kazakov, Y.E., Kublanov, V.S., 2014. Principal Components Method for Heart Rate Variability Analysis. *Biomed. Eng. 48*, 37–41. doi:10.1007/s10527-014-9412-7.

EMOTIV Epoc - 14 Channel Wireless EEG Headset [WWW Document], n.d.. Emotiv. URL https://www.emotiv.com/epoc/ (accessed 9.5.17).

Jolliffe, I., 2014. *Principal Component Analysis, in: Wiley StatsRef: Statistics Reference Online*. John Wiley & Sons, Ltd. doi:10.1002/9781118445112.stat06472.

Kublanov, V., Dolganov, A., Borisov, V., 2016. Application of the discriminant analysis for diagnostics of the arterial hypertension: Analysis of short-term heart rate variability signals. Presented at *the NEUROTECHNIX 2016 - Proceedings of the 4th International Congress on Neurotechnology, Electronics and Informatics, pp. 45–52.*

Kublanov, V.S., Dolganov, A.Y., Belo, D., Gamboa, H., 2017. *Comparison of Machine Learning Methods for the Arterial Hypertension Diagnostics* [WWW Document]. Appl. Bionics Biomech. doi:10.1155/2017/5985479.

Kutilek, P., Charfreitag, J., Hozman, J., 2010. Comparison of Methods of Measurement of Head Position in Neurological Practice, in: *XII Mediterranean Conference on Medical and Biological Engineering and Computing 2010, IFMBE Proceedings*. Springer, Berlin, Heidelberg, pp. 455–458. doi:10.1007/978-3-642-13039-7_114.

Lin, Y.-P., Jung, T.-P., 2017. I*mproving EEG-based emotion classification using conditional transfer learning*. Front. Hum. Neurosci. 11. doi:10.3389/fnhum.2017.00334.

Machado, I.P., Luísa, G., Gamboa, H., Paixão, V., Costa, R.M., 2015. *Human activity data discovery from triaxial accelerometer sensor: Non-supervised learning sensitivity to feature extraction parametrization.* Inf. Process. Manag. 51, 201–214. doi:10.1016/j.ipm.2014.07.008.

Mathie, M., 2003. *Monitoring and Interpreting Human Movement Patterns Using a Triaxial Accelerometer.*

McLachlan, G.J., 1992. *Discriminant Analysis and Statistical Pattern Recognition: McLachlan/ Discriminant Analysis & Pattern Recog, Wiley Series in Probability and Statistics*. John Wiley & Sons, Inc., Hoboken, NJ, USA. doi:10.1002/0471725293.

Mueller, S.T., Piper, B.J., 2014. *The Psychology Experiment Building Language (PEBL) and PEBL Test Battery.* J. Neurosci. Methods 222, 250–259. doi:10.1016/j.jneumeth.2013.10.024.

Okada, Y., Yoto, T.Y., Suzuki, T., Sakuragawa, S., Sugiura, T., 2013. Wearable ECG recorder with acceleration sensors for monitoring daily stress: Office work simulation study. Presented at the *Proceedings of the Annual International Conference of the IEEE Engineering in Medicine and Biology Society, EMBS, pp. 4718–4721.* doi:10.1109/ EMBC.2013.6610601.

Refaeilzadeh, P., Tang, L., Liu, H., 2009. Cross-Validation, in: LIU, L., ÖZSU, M.T. (Eds.), *Encyclopedia of Database Systems*. Springer US, pp. 532–538. doi:10.1007/978-0-387-39940-9_565.

Silva, H.P. da, Fred, A., Martins, R., 2014. Biosignals for Everyone. I*EEE Pervasive Comput. 13, 64–71.* doi:10.1109/MPRV.2014.61.

So, W.K.Y., Wong, S.W.H., Mak, J.N., Chan, R.H.M., 2017. *An evaluation of mental workload with frontal EEG.* PLoS ONE 12. doi:10.1371/ journal.pone.0174949.

Sun, F.-T., Kuo, C., Cheng, H.-T., Buthpitiya, S., Collins, P., Griss, M., 2012. *Activity-aware mental stress detection using physiological sensors. Lect. Notes Inst. Comput. Sci. Soc.-Inform. Telecommun.* Eng. LNICST 76 LNICST, 211–230.

Wolpaw, J., Wolpaw, E.W., 2012. *Brain-Computer Interfaces: Principles and Practice.* Oxford University Press, USA.

Wu, M., Cao, H., Nguyen, H.-L., Surmacz, K., Hargrove, C., 2015. Modeling perceived stress via HRV and accelerometer sensor streams. Presented at the *Proceedings of the Annual International Conference of the IEEE Engineering in Medicine and Biology Society, EMBS, pp. 1625–1628.* doi:10.1109/ EMBC.2015.7318686.

Wu, Y., Miwa, T., Uchida, M., 2017. *Using physiological signals to measure operator's mental workload in shipping–an engine room simulator study.* J. Mar. Eng. Technol. 16, 61–69. doi:10.1080/20464177 .2016.1275496.